Miniaturization of photoacoustic cell for smart endoscope to improve sensitivity

Naoki Wadamori, *Non-member*
a space Department of Electrical, Electronics and Information Engineering
Nagaoka University of Technology
1603-1 Kamitomioka, Nagaoka, Niigata 940-2188 Japan
wadamori@denki.nagaokaut.ac.jp

***Abstract*— Ultrathin endoscopes, such as transnasal endoscopes, have been developed to alleviate discomfort during diagnosis and therapy. However, their application to optional diagnostics is limited since many optional diagnostic instruments are designed to fit through larger side channels. The aim of this study was to develop a smart endoscope that can obtain various diagnoses based on photoacoustic spectroscopy. The photoacoustic process comprises complex energy conversions involving optical, thermal, and elastic processes. This work focused on the scaling potential of photoacoustic sensors. Photoacoustic sensors with two different volumes were developed, and the amplitudes and frequency responses of the photoacoustic signals for silicone rubbers with six different Young's moduli were investigated. The results showed that photoacoustic signals can be enhanced by reducing the volumes of the sensors. Embedding a miniaturized photoacoustic sensor in an endoscope was confirmed to improve the sensitivity.**

I. Introduction

The aim of this study was to develop a smart endoscope to obtain various diagnoses based on photoacoustic (PA) spectroscopy. Whereas conventional transoral endoscopes distinguish between normal tissue and tumors through electronic chromoscopy and endoscopic ultrasound, ultrathin endoscopes such as transnasal endoscopes were developed to alleviate discomfort during diagnosis and therapy. The PA effect produces thermal expansion from the modulated light absorbed by a sample, which generates an acoustic wave. The characteristics of the wave are determined not only by the optical absorption coefficient of the tissue but also by such thermal physical parameters as the thermal expansion, specific heat, and sound velocity. Unlike conventional absorption spectroscopy, the sensitivity of PA spectroscopy scales inversely with the dimensions. Several studies have demonstrated the feasibility of miniaturized PA sensors [1], [2], [3], [4], [5]. The measurement with such sensors, the sample is placed inside a closed chamber called a closed-end PA cell, are not suitable for physiological measurement. For *in vivo* experiments using a PA sensor, the closed state of an open-ended chamber is formed by pressing the bottom of an open-ended chamber to the sample surface. Such detectors are called open-ended PA cells.

*This work was supported by JSPS KAKENHI Grant Number 24680058,24650292.This work has been supported by STARC Grant No. 1340.

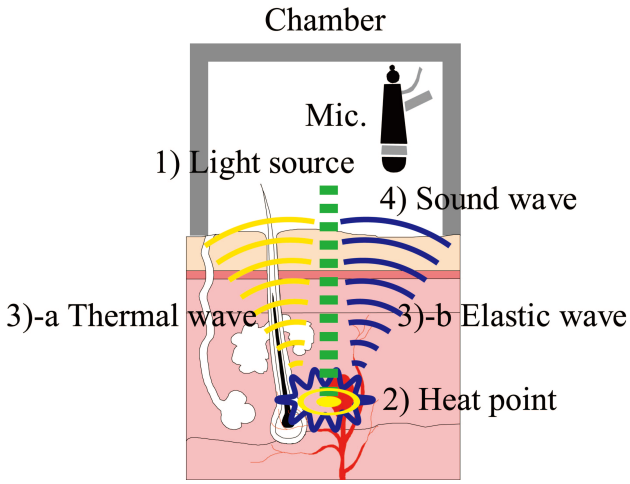

Fig. 1. PA signal–generation mechanisms.

This work focused on the scaling potential of a PA sensor. Open-ended PA cells with different volumes were developed to determine the Young's modulus of a tumor. The amplitudes and frequency responses of PA signals for silicone rubbers with six different Young's moduli were investigated. The experimental results indicated that embedding a miniaturized PA cell in an endoscope improved the sensitivity.

II. Theory

The PA signal–generation mechanisms are shown in Fig.1 [6]. When the sample is illuminated by modulated light, it is heated through non-radiative transitions. This heat generation is also modulated and generates thermal and elastic waves in the sample. These thermal and elastic waves propagate from the region of optical interaction and produce a sound wave to the air from the sample. This sound wave is called the PA signal and is detected by a microphone or piezoelectric device. Therefore, the PA process involves complex energy conversion with optical, thermal, and acoustic processes. Such a generation mechanism for the sound includes surface vibrations sealed in the cavity, as indicated in Fig.2. The initial pressure p_0 in the cavity increases to $p_0 + \delta p$ because of the displacement δx of the diaphragm. This is expressed

978-1-4244-7929-0/14/$26.00 ©2014 IEEE

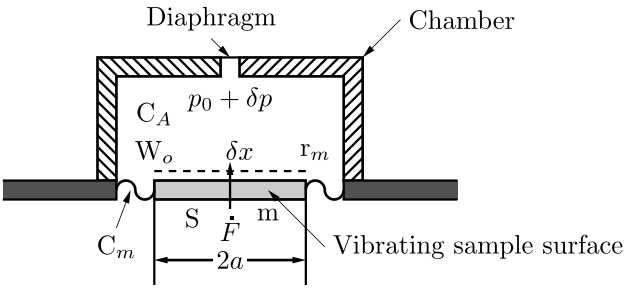

Fig. 2. Equivalent acoustic-mechanical model of PA cell including surface vibration sample.

as follows:

$$\frac{p_0 + \delta p}{p_0} = \left(\frac{W_0}{W_0 - S\delta x}\right)^{\gamma} = 1 + \gamma\frac{S\delta x}{W_0} + \cdots \quad (1)$$

where W_0 is the volume of the cavity, S is the effective area, and γ is the ratio of the specific heat capacity at a constant pressure divided by the specific heat capacity at a constant volume. Thus,

$$\delta p \simeq \frac{p_0\gamma S}{W_0}\delta x \quad (2)$$

This results in the PA effect being enhanced by miniaturization.

III. METHOD

The PA cell comprised a silicon-based microelectromechanical systems (MEMS) microphone and an FSMA-type coupler threaded onto an SMA connector of the emitting fiber (BWF-1540; B&WTEK). The FSMA-type coupler plugged in the SMA connector had a open-ended chamber. When the open-ended chamber was pressed to the sample surface, the open-ended PA cell became a closed-end PA cell. PA cells with chamber heights of 5.3 mm (full size: type F) and 2.4 mm (half size: type H) were made. Schematic views of the PA cells with different heights and the same diameter are presented in Fig.3 and Fig.4, respectively.

The experimental setup in Fig.5 was used to measure the PA signal in the presence of thermoelastic bending of the samples. The laser diode, which had a power of about 34 mW and wavelength of 1550 nm (BWF-1540; B&WTEK) was modulated at the frequency f by a function generator (WF1974; NF Corporation). The PA signal was generated by optical absorption, detected with the MEMS microphone (SPW0430HR5HB-B; Knowles), and transduced to an electric signal amplified with a 40 dB preamplifier (ADA4841-1; Analog Devices). This signal was further amplified with a 36 dB amplifier (PC-SAD8F1-A; SDS) through a low-pass filter (PC-SAD8F1-A; SDS) and processed in a computer after being converted into 16 bits by an A/D converter (PC-G164-1M; SDS). The spot of the laser beam (100 μ m diameter) was directly on the surface of the sample, which was placed on top of the PA cell as shown in Fig.6. Six silicone rubber samples with different Young's moduli (34, 62, 114, 194, 328, and 528 kPa) were investigated using the PA cell in

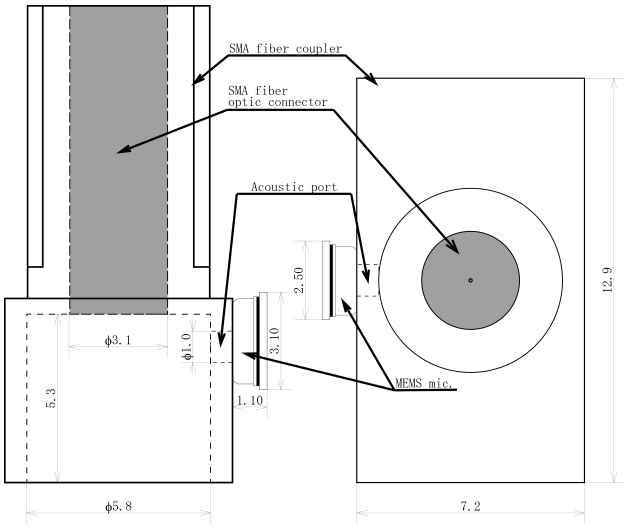

Fig. 3. Schematic view of Type F PA cell for smart endoscope.

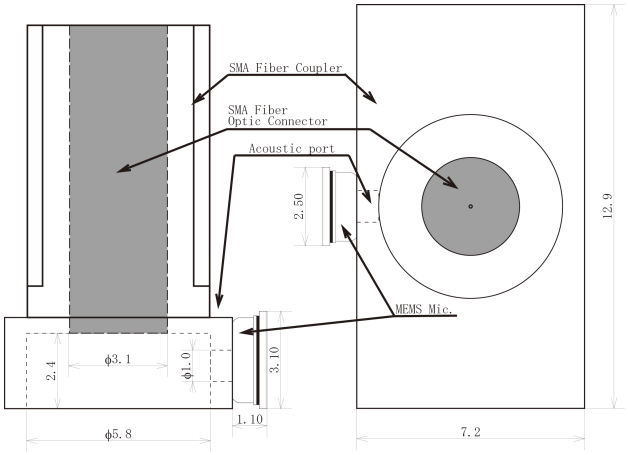

Fig. 4. Schematic view of Type H PA cell for smart endoscope.

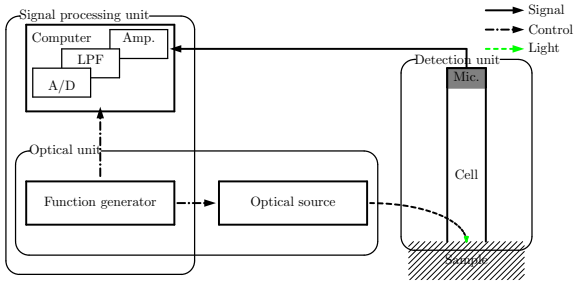

Fig. 5. Diagram of PA system.

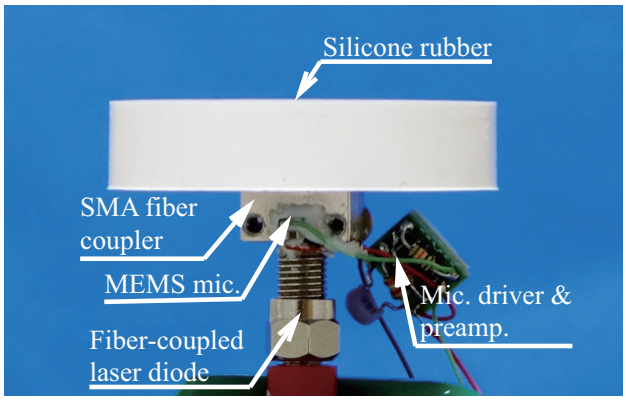

Fig. 6. Photograph of fiber-coupled PA cell and sample on top of PA cell.

TABLE I

PROPERTIES OF SILICONE RUBBERS.

No.	S1	S2	S3
Young's modulus(kPa)	34	62	114
Mass(g)	15.53	15.69	16.43
Diameter(mm)		44	
Thickness(mm)	9.57	9.53	9.58
No.	S4	S5	S6
Young's modulus(kPa)	194	324	528
Mass(g)	16.74	17.15	16.95
Diameter(mm)		44	
Thickness(mm)	9.57	9.58	9.56

this experiment. TABLE I shows the diameters, masses, and thicknesses of the silicone rubber samples.

IV. RESULTS

The amplitude of the PA signal as a function of the modulation frequency is shown in Fig.7, for the six different silicone rubber samples. These amplitudes are the averaged spectrum amplitudes computed by Fourier transform at the modulation frequency. The hollow markers represent type H, and the filled markers represent type F. The behavior of the PA signal amplitude was determined by the superposition of the reciprocal of the modulation frequency with some peaks from the frequency response of the chamber and the sample surface vibration.

The amplitudes of the measured PA signals at the first resonance frequency are given in Fig.8 as a function of the Young's modulus. The hollow circles represent type H, and the hollow triangles represent type F. The amplitudes of the measured PA signals depended on the reciprocal of the modulation frequency.

It can be seen from Fig.7 that the locations of the peak frequency are related to the difference in Young's modules though investigating more deeply.

V. DISCUSSION

Because the sensitivity of the PA spectroscopy scaled inversely with the chamber volume of the PA cell, Fig.8 compares the amplitudes of chambers with different heights. The type H amplitude increased to 3.5 times the type F

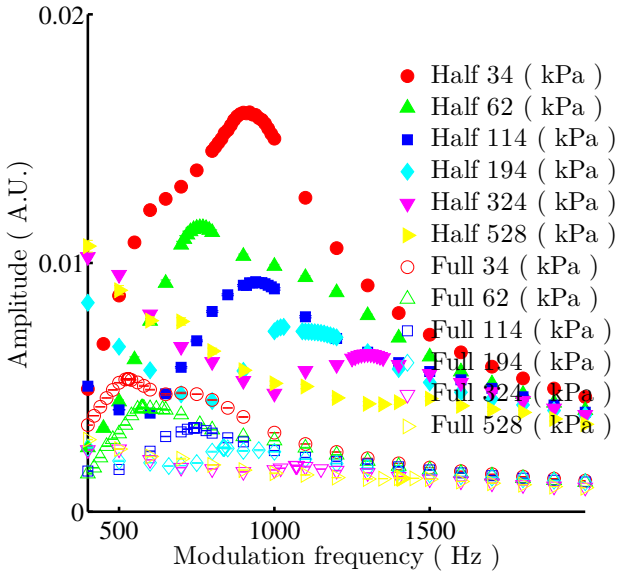

Fig. 7. Amplitude of PA signal measured with type H and F PA cells as function of modulation frequency, for six different silicone rubber samples.

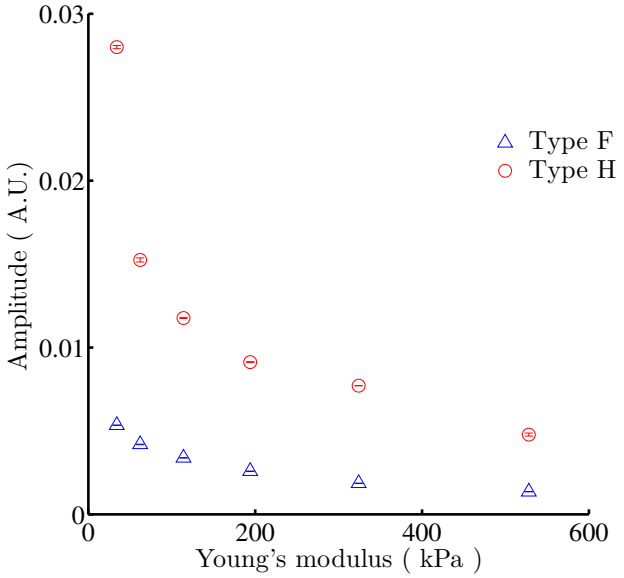

Fig. 8. Amplitude of PA signal measured with type H and F PA cells as function of Young ' s modulus, at first resonance frequency .

amplitude when the Young's modulus was 64–528 kPa; at 32 kPa, it increased to 5.3 times. However these rates of increase were greater than the increases in volume of the type H and type F chambers. The rate of amplitude at 32 kPa differed considerably from the others. The sample was put on the PA cell in an upward direction in order to stabilize the adhesion of the PA cell and sample, as shown in Fig.6. Because the sample was deflected into the chamber of the PA cells, the volume of the chamber decreased. The softest sample at a Young's modulus of 32 kPa was influenced by the type F measurement. This result must be evaluated more carefully from a theoretical point of view by considering other factors. The results confirmed that reducing the volume of the PA cell

improved the sensitivity.

VI. Conclusion

This work evaluated the potential of miniaturized PA cells. The scaling behavior of the PA effect was shown to be empirically proportional to the volume of the chamber. Thus, embedding a miniaturized PA cell in an endoscope should improve the sensitivity. The adhesion method for a sample to a PA cell requires future study. There deserve further study, particularly on real tissue as to its effectiveness on different surfaces with varying absorption processes.

ACKNOWLEDGMENT

This work was supported by JSPS KAKENHI Grant Number 24680058, 24650292. This work has been supported by STARC Grant No. 1340.

References

[1] M. Weber, P. Lerch, and P. Renaud, "Design and simulations of a silicon microfabricated photoacoustic gas sensor," in *MICROSIM II - SIMULATION AND DESIGN OF MICROSYSTEMS AND MICROSTRUCTURES*, vol. 2, 1997, pp. 117–126.

[2] M. Weber, M. Foster, U. Bogli, P. Bachmann, and P. Renaud, "Design and realization of a miniaturized photoacoustic sensor," in *Proc. of Eurosensors XIII*, vol. 13, 1999, pp. 323–326.

[3] S. L. Firebaugh, K. F. Jensen, and M. A. Schmidt, "Miniaturization and integration of photoacoustic detection with a microfabricated chemical reactor system," *J.Microelectromech. Syst.*, vol. 10, no. 2, pp. 232–237, 2001.

[4] ——, "Miniaturization and integration of photoacoustic detection," *J. Appl. Phys.*, vol. 92, no. 3, pp. 1555–1564, 2002.

[5] E. L. Holthoff, D. A. Heaps, and P. M. Pellegrino, "Development of a MEMS-scale photoacoustic chemical sensor using a quantum cascade laser," *IEEE SENSORS*, vol. 10, no. 3, pp. 572–577, 2010.

[6] A. Rosencwaig, *Photoacoustics and photoacoustic spectroscopy*, New York, 1990.